Journal of Engineering Physics and Thermophysics, Vol. 81, No. 5, 2008

NONSTATIONARY HEATING OF TWO-DIMENSIONAL METAL NANOPARTICLES BY LASER RADIATION

S. V. Zimovets[a] and P. I. Geshev[b]

UDC 536.242

A numerical solution of the problem of nonstationary heating of a two-dimensional nanoparticle by laser radiation in the approximation of a constant temperature over the nanoparticle volume is presented. The asymptotes to the heating temperature for long times and for maximum heating of a nanoparticle at long durations of laser radiation have been obtained. It is shown that the temperatures of heating of silver and gold nanoparticles subjected to laser radiation at a resonance wavelength of plasmons are appreciable and may reach the boiling temperature of water.

Introduction. The free electron gas contained inside a metal nanoparticle can be involved in collective vibrational motion when an electromagnetic wave is scattered on the particle. These vibrations of electron plasma are called localized or surface plasmons, since they attenuate exponentially toward the inside of the body. For nanoparticles of noble and alkali metals of size 10–300 nm in the visible part of the spectrum and near IR zone, resonantly enhanced vibrations of plasma — plasmon resonances [1] — can be observed that lead to a multiple increase in the local electromagnetic field on the nanoparticle surface and to resonant enhancement of the extinction and absorption cross sections. A maximum field enhancement factor (FEF) for two-dimensional nanoparticles (nanocylinders) may attain a few tens [2], whereas for three-dimensional nanoparticles the FEF can attain hundreds and even thousands [3, 4].

At the present time, excitation of plasmon resonances is considered to be the major reason for the effect of enhancement of Raman scattering (RS) for the molecules that were adsorbed on microrough metal surfaces (gigantic Raman scattering, GRS [5]) and for colloid solutions of metal nanoparticles [6, 7]. In the latter case, the enhancement factor of GRS for a molecule placed between two metal particles may attain a value of 10^{14} and allows one to record Raman radiation from an individual molecule. This and the fact that for certain nanostructures the field enhancement can be localized in a region measuring less than 10 nm open up wide perspectives for using GRS in biophysics [8].

When a nanoparticle is subjected to laser radiation, a part of the electromagnetic energy is absorbed and the particle and its environment are heated. It is evident that the resonant enlargement of the absorption cross section results in a situation that the temperature of heating of the nanoparticle increases many times as against nonresonant illumination. To use GRS in biophysics, it is extremely important to know what temperatures are attainable in nanoparticles, since strong heating can alter the properties and lead to destruction of organic molecules, as well as to the disturbance of the course of biochemical reactions. Based on plasmon resonances, it is possible to create thermal agents that ensure local heating in the given range of wavelengths and may find application in the solution of a great number of scientific and engineering problems. An example of such particles appears to be dielectric nanoparticles in a metal shell that are successfully used in photothermal therapy of cancer [9, 10].

In what follows we will consider laser-radiation heating of an individual two-dimensional metal nanoparticle placed in a dielectric medium. In such a statement the problem is of no great practical interest, but it allows one to develop the methods of numerical calculation. To solve the problem, we use the ordinary heat-conduction equation (Fourier equation) for a continuous medium. The most interesting cases are those with water or air as the medium surrounding a particle. On the one hand, these media are most abundant, on the other, they have strongly different physical parameters. Therefore the majority of thermophysical calculations considered below were performed precisely for nanoparticles placed in water or air.

[a]Novosibirsk State University, 2 Pirogov Str., Novosibirsk, 630090, Russia; [b]Institute of Thermophysics, Siberian Branch of the Russian Academy of Sciences, 1 Acad. Lavrent'ev Ave., Novosibirsk, 630090, Russia. Translated from Inzhenerno-Fizicheskii Zhurnal, Vol. 81, No. 5, pp. 936–943, September–October, 2008. Original article submitted May 25, 2006; revision submitted March 6, 2008.

We will consider the question of the validity of the equations of a continuous medium for nanoparticles. For the medium surrounding the particle to be considered continuous, it is necessary that the mean free path l in the medium be much smaller than the characteristic dimension of the nanoparticle ($l << L$). For air under normal conditions l is equal to about 60 nm [11] and, consequently, in air the continuous medium approximation is applicable only to nanoparticles of size $L >> 60$ nm. The space between the water molecules is of the same order of magnitude as the size of the molecule, that is, of several angstroms. In this case too, for nanoparticles of size greater than 10 nm the continuous medium approximation holds.

We note that the problems related to thermal processes in nanostructures were solved in [12–16]. Among works closest to the topic considered are [12, 13], where the problem of heating a scanning tunnel microscope needle is tackled. But the influence of the enhancement of the field at the needle tip on the heating of the needle is less substantial, since the needle is the macroobject and heat spreads rapidly over the large volume. In [14–16], the processes of heat transfer and heat release by radiation are studied. As far as the authors know, at the present time there are no investigations devoted to nonstationary heating of nanoparticles placed in a medium.

Two-Dimensional Problem of Nonstationary Heat Conduction. We will consider a two-dimensional particle with the characteristic dimension L placed in an external medium and subjected to laser radiation. It is assumed that the medium surrounding the particle is transparent, i.e., the relative permittivity of the medium ε_e is the real quantity ($\mathrm{Im}[\varepsilon_e] = 0$) and there is no heat release in the medium ($Q_e = 0$). According to the classical electrodynamics, for volumetric heat generation inside the nanoparticle we may write $Q_p = -(\nabla' \cdot \mathbf{S})$. Having averaged over the volume, for the average density of heat generation inside the nanoparticle we obtain $\overline{Q}_p = \sigma' I / V'$, where $\sigma' = -\oint\limits_{\Gamma'} (\mathbf{S} \cdot \mathbf{n}) / I d\Gamma'$.

It is known that in a two-dimensional case the problem of heat conduction has no stationary solution in an infinite space. Therefore we will consider only laser radiation pulses limited in time with the characteristic time τ, and as the time dependence we take the Gaussian function $I = I_0 \exp(-(t'/\tau)^2)$. The temperature distribution in the medium is described by the heat conduction equation

$$C \partial T / \partial t' = \nabla' (\lambda \nabla' T) + Q . \tag{1}$$

We will consider that the heat capacity C and thermal conductivity λ are homogeneous throughout the particle volume and environment volume and are independent of temperature. All the thermophysical quantities used in the calculations were taken from [17]. We introduce the dimensionless variables

$$t = t'/\tau , \quad x = x'/L , \quad y = y'/L , \quad \theta = (T - T_0)/(\sigma T_*) , \quad q = Q/\overline{Q} . \tag{2}$$

Then, if there is no heat generation in the environment, we may write

$$\mathrm{Fo}_p \Delta\theta_p - \frac{\partial \theta_p}{\partial t} = -\frac{q_p \exp(-t^2)}{\sqrt{\pi}} , \quad \mathrm{Fo}_e \Delta\theta_e - \frac{\partial \theta_e}{\partial t} = 0 . \tag{3}$$

We will define the Fourier transformation as follows:

$$\tilde{f}(\omega) = \int\limits_{-\infty}^{\infty} f(t) \exp(i\omega t)\, dt , \quad f(t) = \frac{1}{2\pi} \int\limits_{-\infty}^{\infty} \tilde{f}(\omega) \exp(-i\omega t)\, d\omega \tag{4}$$

and apply it to system (3):

$$\mathrm{Fo}_p \Delta\tilde{\theta}_p + i\omega\tilde{\theta}_p = -q_p \exp\left(-(\omega/2)^2\right) , \quad \mathrm{Fo}_e \Delta\tilde{\theta}_e + i\omega\tilde{\theta}_e = 0 . \tag{5}$$

Averaging of the first equation of system (5) over the cross-sectional area of the particle and using the continuity of the heat flux through the boundary yield an equation for the average temperature of the particle in the Fourier representation:

$$\bar{\tilde{\theta}}_{\mathrm{p}} = -\frac{\exp\left(-(\omega/2)^2\right)}{\chi \mathrm{Fo}_{\mathrm{e}}\,\Psi + i\omega}, \quad \Psi = \frac{1}{V}\oint_{\Gamma}\frac{\partial\psi}{\partial n}\,d\Gamma, \quad \chi = \frac{C_{\mathrm{e}}}{C_{\mathrm{p}}}, \tag{6}$$

where $\frac{\partial\psi}{\partial n}$ is the derivative over the normal to the body surface of the function $\psi = \tilde{\theta}_{\mathrm{e}}/\bar{\tilde{\theta}}_{\mathrm{p}}$, the equation for which results from the division of the second equation of system, (5) by $\bar{\tilde{\theta}}_{\mathrm{p}}$:

$$\Delta\psi + k_{\mathrm{e}}^2\psi = 0, \quad \psi|_{\infty} = 0, \quad \psi|_{\Gamma} = \tilde{\Theta}, \quad \tilde{\Theta} = \tilde{\theta}_{\mathrm{p}}|_{\Gamma}/\bar{\tilde{\theta}}_{\mathrm{p}}. \tag{7}$$

Equation (7) together with the boundary conditions is not closed, since the boundary conditions contain the unknown function $\tilde{\Theta}$. But if this function is known, then by having solved Eq. (7) and taken the inverse Fourier transform of Eq. (6), we may find the average temperature of the heating of the particle at any instant of time:

$$\bar{T}_{\mathrm{p}} = T_*\sigma\bar{\theta}_{\mathrm{p}}, \quad \bar{\theta}_{\mathrm{p}} = -\frac{1}{\pi}\,\mathrm{Re}\left[\int_0^{\infty}\frac{\exp\left(-(\omega/2)^2 - i\omega t\right)}{\chi \mathrm{Fo}_{\mathrm{e}}\,\Psi + i\omega}\,d\omega\right]. \tag{8}$$

Approximation of the Temperature Homogeneous over the Particle Volume. We will consider laser radiation pulses the duration of which considerably exceeds the characteristic time of the inner problem. In this case, the temperature distribution inside the particle is independent of the distribution of heat sources, and the temperature is virtually homogeneous over the particle volume. The extent of inhomogeneity is proportional to the ratio of thermal conductivities $\lambda_{\mathrm{e}}/\lambda_{\mathrm{p}}$. The thermal conductivity of metals is a high value and for the majority of media surrounding the particle we may consider that $\Theta = \theta_{\mathrm{p}}|_{\Gamma}/\bar{\theta}_{\mathrm{p}} \approx 1$, i.e., the temperature is homogeneous over the nanoparticle volume (the approximation of the homogeneous temperature of the particle — HTP). The condition $\tau >> \tau_{\mathrm{p}}$ can be written in a form restricted to two dimensionless parameters of the problem:

$$\chi \mathrm{Fo}_{\mathrm{e}} >> \lambda_{\mathrm{e}}/\lambda_{\mathrm{p}}. \tag{9}$$

Adopting this restriction and using the Green identity, Eq. (7) together with the boundary conditions can be transformed into the boundary integral equation

$$\oint_{\Gamma}\frac{\partial\psi}{\partial n}\,G\,d\Gamma = \oint_{\Gamma}\frac{\partial G}{\partial n}\,d\Gamma - \frac{1}{2}, \tag{10}$$

where $G(\mathbf{r}, \mathbf{r}_0) = (i/4)H_0^{(1)}\left(k_{\mathrm{e}}|\mathbf{r} - \mathbf{r}_0|\right)$ is the Green function of the Helmholz two-dimensional equation, $\mathbf{r}_0 = (x_0, y_0)$ and $\mathbf{r} = (x, y)$ are the points of observation and integration, respectively.

Equation (10) can be solved numerically with the aid of the method of boundary elements [2], and it allows one to find the boundary values of the function $\partial\psi/\partial n$ for particles of arbitrary shape. Thereafter, using (8), we can calculate the average temperature of the nanoparticle at any instant of time.

We note that in the HTP approximation the material from which the particle consists is characterized only by its volumetric heat capacity C_{p}. For different metals the value of volumetric heat capacity in units MJ/(m^3·K) is equal to 2.52 (Ag), 2.51 (Au), 6.47 (K), 1.19 (Na), 2.78 (Zn), 2.79 (Pt), 3.49 (Cu), and 3.92 (Ni). It is seen that the scatter of the values is not large for the majority of metals (for gold and solver it is practically zero). Consequently, the results of calculations carried out for one of the metals (Ag) can be adopted with a certain accuracy also for other metals (Au, Zn, Pt, Cu, and Ni). In what follows, the majority of calculations of the heat conduction problem will be performed for silver particles placed in water and air.

Heating of Cylindrical Particles. For cylindrical particles the problem admits an analytical solution. We will consider two limiting cases: uniform heat release over the particle volume and heat release only on the particle boundary. As before, the average temperature is determined by Eq. (6), and in the case of uniform heat release the functions $\tilde{\Theta}$ and Ψ are

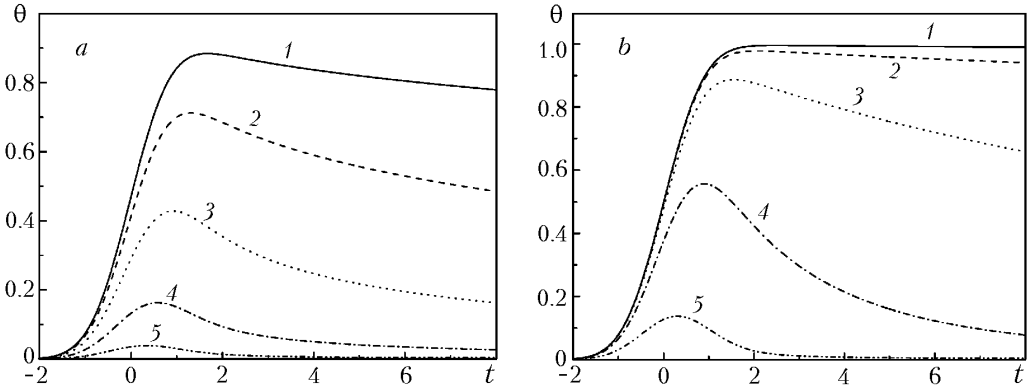

Fig. 1. Function $\bar{\theta}_p$ depending on time for a circular silver cylinder placed in water (a) and air (b): curves 1–5 correspond to $\chi Fo_e = 10^{-3}$, 10^{-2}, 10^{-1}, 1, 10.

$$\tilde{\Theta} = \left[1 + \frac{1}{i\omega}\left(\frac{k_p J_0(k_p)}{2J_1(k_p)} - 1\right)\chi Fo_e \Psi_0\right]^{-1}, \quad \Psi = \tilde{\Theta}\Psi_0, \tag{11}$$

in the case of heat release on the boundary

$$\tilde{\Theta} = \frac{k_p J_0(k_p)}{2J_1(k_p)}, \quad \Psi = \tilde{\Theta}\Psi_0, \tag{12}$$

where Ψ_0 is the solution for a circular cylinder in the approximation of a homogeneous temperature of the particle:

$$\Psi_0 = -\frac{2k_e H_1^{(1)}(k_e)}{H_0^{(1)}(k_e)}. \tag{13}$$

A comparison was carried out between the analytical solutions calculated with the aid of Eqs. (11) and (12) and the solutions in the HTP approximation obtained by numerical calculation of Eq. (10). The relative deviation was determined from the formula $\delta = \max\limits_{t \in [-2;8]} [(\bar{\theta}_p(t) - \bar{\theta}_p^*(t))/\bar{\theta}_p^*(t)]$, where $\bar{\theta}_p^*$ is one of the two analytical solutions. The particle radius was taken as the characteristic dimension L. For a particle placed in water δ does not exceed 2% at $\chi Fo_e > 10^{-3}$ and for particles in air — at $\chi Fo_e > 10^{-5}$.

Analysis and Results of Calculations of Dimensionless Temperature. It is clear that the function $\bar{\theta}_p$ is limited. On the one hand, it cannot be smaller than zero, and, on the other hand, it cannot exceed unity, since the quantity T_* is the increment of the temperature of the thermally insulated particle. We will designate the temperature maximum in time by $\bar{\theta}_{max}$. The maximum will tend to unity at small values of τ ($\tau << \tau_e/\chi$, $\chi Fo_e << 1$), since in this case the particle has no time to give up heat during the time of laser pulse action. This is seen in Fig. 1, where the results of calculations for a cylindrical silver nanoparticle placed in water and air at different values of the parameter χFo_e are presented. The value $\chi Fo_e = 10^{-3}$ does not satisfy the condition of applicability of the HTP approximation (9), but vividly demonstrates the saturation of the maximum of the function $\bar{\theta}_p$.

In the reverse case, when the value of τ is large ($\chi Fo_e >> 1$), the environment effectively removes heat, $\bar{\theta}_{max} << 1$, and the position of the maximum in time tends to maximum heat release ($t = 0$). To find the asymptotics of the function $\bar{\theta}_{max}$ at $\chi Fo_e >> 1$, we note that in time $t > 1/Fo_e$ heat penetrates into the medium to a great distance and a temperature distribution close to a cylindrically symmetric one is formed around the particle. Therefore the value of $\bar{\theta}_{max}$ at high values of Fo_e will weakly depend on the shape of a nanoparticle, and the asymptotics calculated for

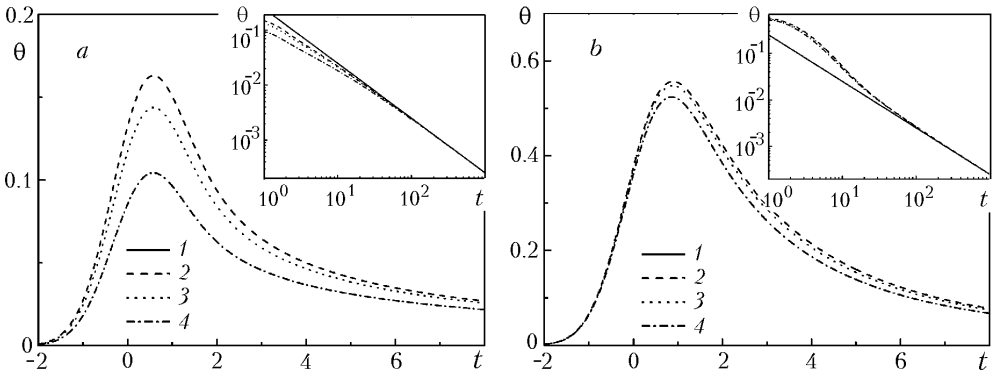

Fig. 2. Function $\bar{\theta}_p$ at $\chi Fo_e = 1$ depending on time for an elliptic silver cylinder placed in water (a) and air (b): 1) asymptotics (15) for large times; 2, 3, 4) a particle with the ratio of semiaxes A/B = 1, 3, 9.

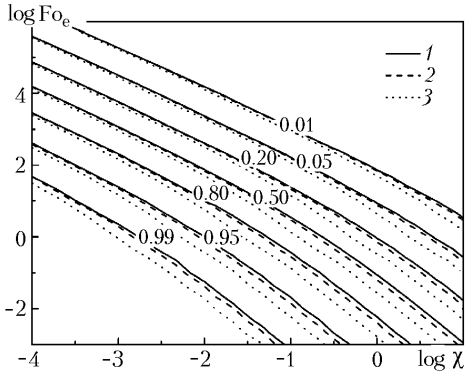

Fig. 3. Chart of the lines of the level of temperature maximum $\bar{\theta}_{max}$ for a silver elliptical cylinder: 1, 2, 3) for the ratios of semiaxes A/B = 1, 3, 9. Figures at the curves give the value of dimensionless maximum temperature.

the circular cylinder will also be the asymptotics for particles of arbitrary shape but of the same cross-sectional area. We will substitute into Eq. (8) the expansion of function (13) in small k_e, assume that $t = 0$, and omit the terms proportional to k_e^2 and k_e^2/χ. Having calculated the integral, we obtain

$$\bar{\theta}_{max} = \frac{\ln Fo_e}{4\sqrt{\pi\,\chi Fo_e}}, \quad Fo_e >> 1, \quad \chi Fo_e >> 1. \tag{14}$$

The asymptotics (14) describes the numerical results with an accuracy better than 10% at min [Fo_e, χFo_e] > 100. The checking was carried out for a silver elliptical nanoparticle, with the semiaxes ratio A/B from 1 to 9, placed in water and air. When the shape of the particle is close to a cylindrical one, in the numerator of Eq. (14) one can preserve the constant equal to $2(0.491 - c) + \ln 2$ (c is the Euler constant), which considerably improves the accuracy of the asymptotics for such particles.

At long times the integrand in Eq. (8) oscillates rapidly and it is difficult to perform its numerical calculation. We will find its asymptotics for a circular cylinder. As shown above, it will also be the asymptotics for particles of arbitrary shape at $t > 1/Fo_e$. The major portion of the integral in (8) at $t >> 1$ will be integrated at small values of ω. Neglecting terms proportional to k_e^2 and k_e^2/χ, we obtain

$$\bar{\theta}_p = \frac{1}{4\chi Fo_e t}, \quad t >> \frac{1}{Fo_e}, \quad t >> \frac{1}{\chi Fo_e}. \tag{15}$$

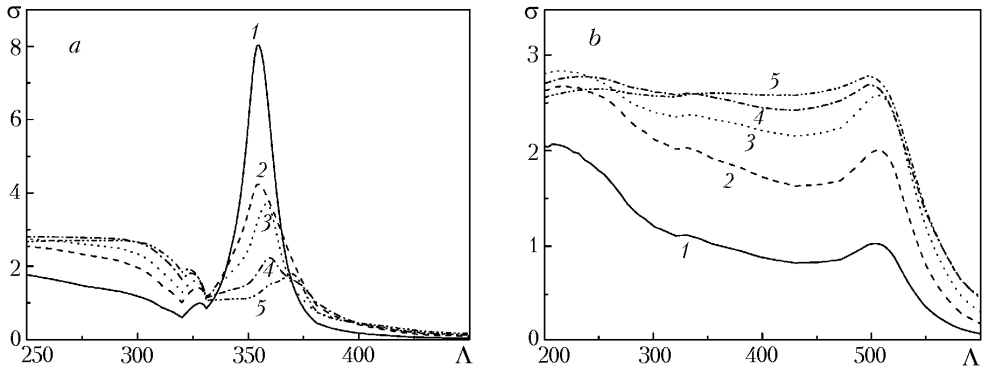

Fig. 4. Dependence of σ on the wavelength Λ for a silver (a) and gold (b) cylindrical nanoparticle placed in water: 1–5) particle radius L = 10, 20, 30, 50, and 70 nm. Λ, nm.

The dependence of temperature on time for different elliptical silver cylinders is shown in Fig. 2. On the insets the temperature is compared with asymptotics (15). Figure 3 presents the picture of the lines of the level of the function $\bar{\theta}_{\max}$ depending on two dimensionless parameters of the problem $\mathrm{Fo_e}$ and χ. The picture allows the conclusion that the particle can be considered thermally insulated in a wide range of the parameters χ — $[10^{-4}, 10]$ at $\chi^5 \mathrm{Fo_e}^3 < 10^{-14}$. Knowing the absorption cross section of the nanoparticle, its thermophysical properties, the properties of the environment, as well as the parameters of the laser pulse, one can easily determine the temperature of the maximum heating of the nanoparticle with the aid of Fig. 3.

From the results of numerical calculation the following approximating formula was obtained for a circular cylinder:

$$\bar{\theta}_{\max}(\mathrm{Fo_e}, \chi) = \frac{1}{1 + 4.47 \mathrm{Fo_e}^{b} \chi^{c}}, \quad b = 0.67 + 0.04 \cdot \log(\mathrm{Fo_e}) - 0.0019 \cdot \log(\mathrm{Fo_e})^2,$$

$$c = 0.97 + 0.0072 \cdot \log(\mathrm{Fo_e}), \tag{16}$$

which describes the lines of the level of the surface shown in Fig. 3 with an error not higher than 10%.

Temperature of Heating of Metal Particles by Laser Radiation. To calculate the temperature of heating of nanoparticles, it is necessary to know the laser radiation absorption section. The sections were obtained by solving the total Maxwell equations by the method given in [2]. For nanoparticles larger than 10 nm the influence of the additional damping due to the scattering of electrons on the nanoparticle surface can be ignored [18]. Therefore in calculations the bulk dielectric permeability obtained for the nanoparticle substrate in optical experiments [19] is used. The electromagnetic wave incident on the particle has the transverse electric (TE) polarization (when the electric field vector and the wave vector are perpendicular to the particle generatrices, i.e., they lie in the x–y plane). The transverse magnetic (TM) polarization (when the magnetic field vector lies in the x–y plane) does not entail excitation of plasmon resonances and therefore is of no interest.

Figure 4 depicts the absorption cross sections (normalized to the characteristic dimension of the particle L) for cylindrical silver and gold nanoparticles placed in water. The nanoparticle radius was used as the characteristic dimension. The sections of silver nanoparticles demonstrate a clearly seen resonance behavior. A maximum value of the normalized absorption cross section is observed for fine particles. When they increase in size, the magnitude of the resonance decreases and a small displacement to the longwave region occurs. In the case of gold nanoparticles, there are no clearly visible plasmon resonances. The reason is that the imaginary part of the relative dielectric permeability of gold in the range of wavelengths Λ — [300, 500] nm is not high $\left(\mathrm{Im}\left|\varepsilon_{\mathrm{p}}\right| \approx 6\right)$, and the resonance is strongly suppressed.

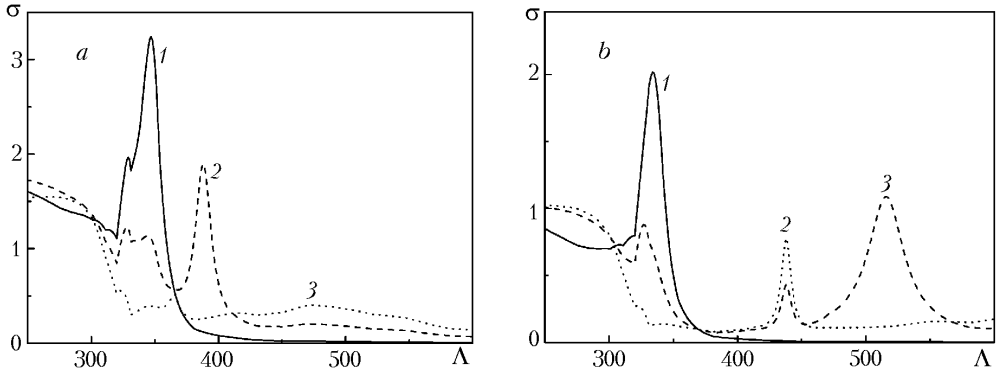

Fig. 5. Dependence of σ on the wavelength Λ for a silver elliptical nanoparticle placed in water: a) ratio of semiaxes A/B = 3; b) 9; $L = \sqrt{A/B}$ = 30 nm; 1, 2, 3) φ = 0°, 45°, and 90°. Λ, nm.

With air being the medium that surrounds a particle, the solution suggested is applicable only to particles with $L >> 60$ nm. For relatively large ($L > 50$ nm) two-dimensional nanoparticles the resonance in the absorption cross-section spectrum is weakly expressed and cannot lead to a substantial increase in the temperature of nanoparticle heating as compared to nonresonant illumination. This is seen from Fig. 4. In air the absorption spectra behave similarly, but the resonance is displaced to the shortwave region. Therefore the heating temperatures are calculated only for the nanoparticles that were placed in water.

We will determine the temperature of the heating of nanoparticles on excitation of plasmon resonances in them. At I_0 = 1 MW/cm^2 and τ = 10 nsec ($W \approx 18$ mJ/cm^2) the characteristic temperature for silver and gold is equal to $T_* \approx 2.24 \cdot 10^4/L$, where L is in nanometers. The calculation of the value of $\bar{\theta}_{max}$ for different radii L = 10, 20, 30, 50, and 70 nm yields $T_* \bar{\theta}_{max} \approx$ 46, 62, 69, 74, and 74 K, respectively. Having multiplied by the resonant maxima of cross sections, we obtain maximum temperatures of heating: $\bar{T}_p \approx$ 370, 262, 257, 166, and 133 K for a silver nanoparticle and $\bar{T}_p \approx$ 49, 128, 185, 207, and 214 K for a gold nanoparticle.

For particles that do not have a cylindrical shape, the position and the magnitude of resonances depend substantially on both the shape of a nanoparticle and direction of illumination. Figure 5 demonstrates normalized absorption cross sections for an elliptical silver nanoparticle with different ratios of semiaxes (A/B = 3 and 9) and with the characteristic dimension $L = \sqrt{AB}$ = 30 nm. The particle was illuminated at angles φ = 0°, 45°, and 90° to the large semiaxis of the elliptical cylinder. The absorption cross sections calculated at a fixed wavelength may differ substantially for different illumination angles. For example, for the resonance at the wavelength Λ = 516 nm (Fig. 5b) the section corresponding to the illumination angle φ = 45° exceeds by more than 320 times the absorption cross section at φ = 0°. As follows from Eq. (8), the temperature of heating for these two angles will differ by the same number of times.

Conclusions. The problem of heating of a single metal nanoparticle by laser radiation has been solved in the approximation of the temperature which is homogeneous over the nanoparticle volume. It is shown that this approximation ensures a sufficient accuracy in a wide range of dimensionless parameters of the problem. To solve the problem, the method of boundary integral equations has been used, which is substantially advantageous over the grid methods: Only the values of the quantities at the body boundary are calculated, i.e., the two-dimensional problem has been reduced to a one-dimensional one, and the temperature field around the particle can be calculated from the boundary values. Therefore the method allows one to easily calculate the heating temperature of nanoparticles at long times and laser radiation pulse durations. The use of grid methods at such parameters would have led to the necessity of constructing a grid in a large volume of the medium surrounding the particle.

For the dimensionless temperature of the heating of a particle ($\bar{\theta}_p$) an asymptote has been obtained at long times and for the maximum of this temperature in time ($\bar{\theta}_{max}$) — the asymptote at long laser radiation pulses. For a circular cylinder, an approximation formula has been obtained; it describes the function $\bar{\theta}_{max}$ at χ — [10^{-4}, 10], Fo_e — [10^{-3}, 10^6] with an error not exceeding 10%. It is shown that at values $\chi^5 Fo_e^3 < 10^{-14}$ metal particles can be considered practically thermally insulated ($\bar{\theta}_{max} \approx 1$) within the range χ — [10^{-4}, 10].

The temperatures of heating of cylindrical silver and gold particles placed in water on excitation of plasmon resonances in them have been calculated. For laser radiation with $I_0 = 1$ MW/cm^2 and $\tau = 10$ nsec ($W \approx 18$ mJ/cm^2) the heating temperatures of silver and gold nanoparticles measuring 10–70 nm lie in the range 50–370 K. The heating temperatures are proportional to the integral density of laser radiation energy $W = \sqrt{\pi} I_0 \tau$ and with a change in these parameters (W or I_0, or τ) the calculated temperatures of heating change proportionally. Consequently, the heating of nanoparticles is appreciable, and for a complete understanding of the processes occurring in the course of laser irradiation of particles it should be taken into account. For example, almost all calculated heating temperatures exceed the boiling point of water.

It is shown that for nanoparticles with an elliptic cross section the heating temperatures at different angles of illumination may differ by several hundreds of times.

It should be noted that the problem has been solved in dimensionless form, and consequently, the solution can be applied not only to nanoparticles but also to problems of heating of two-dimensionless bodies of arbitrary size provided that condition (9) that expresses the constancy of temperature over the body volume holds.

NOTATION

A, B, large and small semiaxes of an elliptical cylinder, m; a, thermal diffusivity, $a = \lambda/C$, m^2/sec; C, volumetric heat capacity at constant pressure, J/(K·m^3); Fo, Fourier number, Fo $= a\tau/L^2$; $H_n^{(1)}$, Hankel function of the first kind and nth order; I, laser radiation power density, W/m^2; I_0, maximum of laser radiation power density, W/m^2; i, imaginary unit; J_n, Bessel function of nth order; k, wave vector of the problem in Fourier presentation, $k = \sqrt{i\omega/\mathrm{Fo}}$; l, free path, m; L, characteristic dimension of a particle, for elliptical particles $L = \sqrt{AB}$, m; $\mathbf{n}$, outer normal to the particle boundary; Q, density of volumetric sources of heat release, W/m^3; $\mathbf{S}$, time-averaged Poynting vector; q, dimensionless density of volumetric sources of heat release; T, temperature, K; T_0, initial temperature of a particle and of the environment, K; T_*, characteristic temperature of the problem, $T_* = W/(LVC_\mathrm{p})$, K; t, dimensionless time; V, dimensionless cross-sectional area of the particle; W, density of the energy obtained by the particle in the course of action of a laser pulse, J/m^2; x, y, dimensionless Cartesian coordinates; Γ, particle boundary; ε, permittivity; Θ, boundary values of relative temperature, $\tilde{\Theta} = \psi|_\Gamma$; Λ, laser radiation wavelength, m; λ, thermal conductivity, W/(K·m); σ, dimensionless cross section of absorption of laser radiation by a particle; σ', absorption cross section of a nanoparticle; τ, characteristic time of a laser pulse, sec; τ_e, τ_p, characteristic time of outer and inner problems, $\tau_{\mathrm{e,p}} = L^2/a_{\mathrm{e,p}}$, sec; φ, angle between the large semiaxis of an elliptical particle and direction of illumination; χ, ratio of volumetric heat capacities of environment and particle; Ψ, total relative heat flux through the particle boundary; ψ, relative temperature of heating of the environment; ω, frequency, Fourier-image variable. Subscripts and superscripts: e, environment; p, particle; max, maximum value in time; $\tilde{}$, Fourier representation; overbar, volume averaging; $'$, not dimensionalized space and time quantities except for L, τ, τ_e, τ_p.

REFERENCES

1. C. F. Bohren and D. R. Huffman, *Absorption and Scattering of Light by Small Particles* [Russian translation], Mir, Moscow (1986).
2. S. V. Zimovets and P. I. Geshev, Method of boundary integral equations for calculating the scattering of light on two-dimensional nanoparticles, *Zh. Tekh. Fiz.*, **76**, No. 3, 1–6 (2006).
3. P. I. Geshev, S. Klein, T. Witting, K. Dickmann, and M. Hietschhold, Calculation of the electric-field enhancement at nanoparticles of arbitrary shape in close proximity to a metallic surface, *Phys. Rev. B*, **70**, 075402–16 (2004).
4. P. I. Geshev and K. Dickmann, Enhanced radiation of a dipole placed between a metallic surface and a nanoparticle, *J. Opt. A: Pure Appl. Opt.*, **8**, 161–173 (2006).
5. M. Moskovits, Surface-enhanced spectroscopy, *Rev. Mod. Phys.*, **57**, No. 3, Pt. 1, 783–826 (1985).
6. K. Kneipp, Y. Wang, H. Kneipp, I. Itzkan, R. Dasari, and M. S. Feld, Population pumping of excited vibrational states by surface-enhanced Raman scattering, *Phys. Rev. Lett.*, **76**, 2444–2447 (1996).

7. S. Nie and S. R. Emory, Probing single molecules and single nanoparticles by surface-enhanced Raman scattering, *Science*, **275**, 1102–1106 (1997).
8. K. Kneipp, H. Kneipp, I. Itzkan, R. R. Dasari, and M. S. Feld, Surface-enhanced Raman scattering and biophysics, *J. Phys.*, **14**, 597–624 (2002).
9. D. P. O'Neal, L. R. Hirsch, N. J. Halas, and J. D. Payne, Photo-thermal tumor ablation in mice using infrared-adsorbing nanoparticles, *Cancer Lett.*, **209**, 171–176 (2004).
10. L. R. Hirsch, A. M. Gobin, A. R. Lowery, R. A. Drezek, N. J. Halas, and J. L. West, Metal nanoshells, *Annals Biomed. Eng.*, **34**, No. 1, 15–22 (2006).
11. L. A. Bird, *Molecular Gas Dynamics* [Russian translation], Mir, Moscow (1981).
12. P. I. Geshev, S. Klein, and K. Dickmann, Calculation of the temperature and thermal expansion of an STM tip heated by a short laser pulse, *Appl. Phys. B*, **76**, 313–317 (2003).
13. A. Downes, D. Salter, and A. Elfick, Heating effects in tip-enhanced optical microscopy, *Opt. Exp.*, **14**, No. 12, 5216–5222 (2006).
14. A. I. Volokitin and B. N. J. Persson, Radiative heat transfer between nanostructures, *Phys. Rev. Lett.*, **63**, 205404–11 (2001).
15. G. Domingues, S. Voltz, K. Joulain, and J.-J. Greffet, Heat transfer between two nanoparticles through near field interaction, *Phys. Rev. Lett.*, **94**, 85901–4 (2005).
16. Yu. V. Martynenko and L. I. Ognev, Thermal radiation of nanoparticles, *Zh. Tekh. Fiz.*, **75**, No. 11, 130–132 (2005).
17. A. Ya. Guva, *Brief Thermophysical Handbook* [in Russian], Sibvuzizdat, Novosibirsk (2002).
18. M. Quinten, Optical constant of gold and silver clusters in the spectral range between 1.5 eV and 4.5 eV, *Z. Phys. B*, **101**, 211–217 (1996).
19. E. Palik, *Handbook of Optical Constants of Solids*, Academic Press, New York (1985).